nature neuroscience

SUPPLEMENTARY INFORMATION

https://doi.org/10.1038/s41593-018-0162-9

In the format provided by the authors and unedited.

Optimization of interneuron function by direct coupling of cell migration and axonal targeting

Lynette Lim[1,2,3], Janelle M. P. Pakan[4,6,7], Martijn M. Selten[1,2,7], André Marques-Smith[1,2], Alfredo Llorca[1,2], Sung Eun Bae[1,2], Nathalie L. Rochefort[4,5] and Oscar Marín[1,2,3]*

[1]Centre for Developmental Neurobiology, Institute of Psychiatry, Psychology and Neuroscience, King's College London, London, UK. [2]MRC Centre for Neurodevelopmental Disorders, King's College London, London, UK. [3]Instituto de Neurociencias, Consejo Superior de Investigaciones Científicas & Universidad Miguel Hernández, Sant Joan d'Alacant, Spain. [4]Centre for Integrative Physiology, School of Biomedical Sciences, University of Edinburgh, Edinburgh, UK. [5]Simons Initiative for the Developing Brain, University of Edinburgh, Edinburgh, UK. [6]Present address: Center for Behavioral Brain Sciences, Institute of Cognitive Neurology and Dementia Research, German Center for Neurodegenerative Diseases, Otto-von-Guericke University, Magdeburg, Germany. [7]These authors contributed equally: Janelle M. P. Pakan, Martijn M. Selten. *e-mail: oscar.marin@kcl.ac.uk

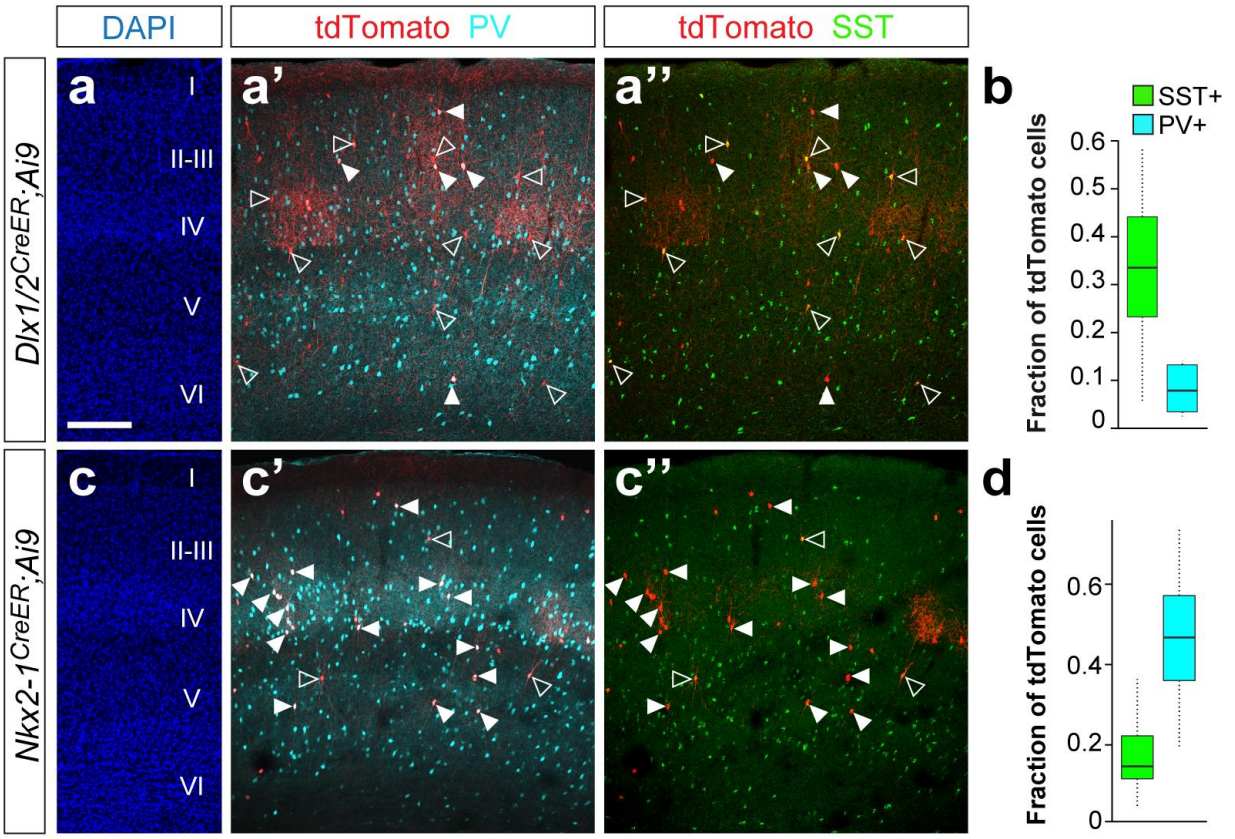

Supplementary Figure 1

PV^{+} and SST^{+} interneurons in *Dlx1/2^{CreER}* and *Nkx2-1^{CreER}* mouse lines.

(**a,c**) Coronal sections through the somatosensory cortex of P30 *Dlx1/2^{CreER};Ai9* (**a**) and *Nkx2-1^{CreER};Ai9* (**c**) showing the distribution of TdTomato cells that also express PV or SST. Open arrowheads point to TdTomato-expressing cells that do not express PV (**a',a"**) or SST (**c',c"**), whereas arrowheads indicate TdTomato/PV (**a',a"**) and TdTomato/SST (**c',c"**) double-labeled cells, repeated with similar results over 3 animals. (**b,d**) Boxplots represent median, 1st and 3rd quartile, and 1.5 IQR for fraction of TdTomato/PV and TdTomato/SST double-labeled cells in *Dlx1/2^{CreER};Ai9* (**b**) and *Nkx2-1^{CreER};Ai9* (**d**) mice. *n* = 3 mice per genotype. Scale bar equals 100 µm.

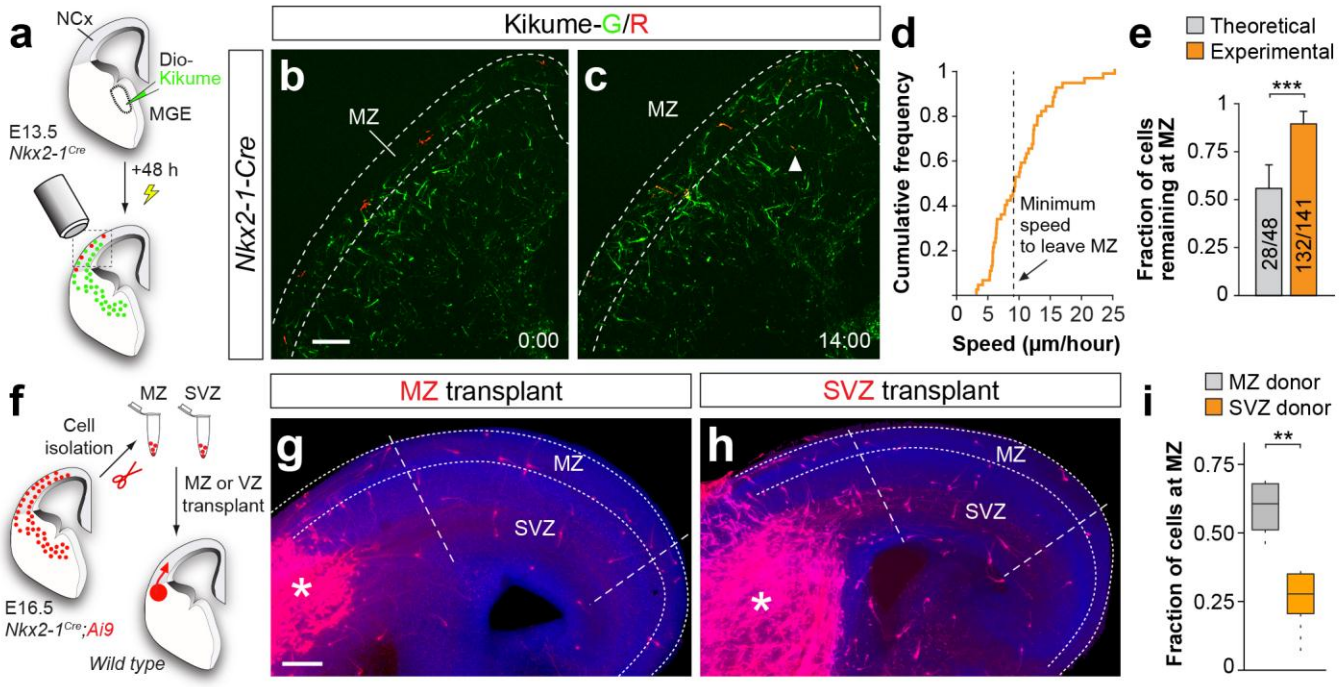

Supplementary Figure 2

Early commitment to migratory routes by MGE-derived interneurons.

(**a**) Schematic of experimental design for the imaging of Kikume Green-Red labeled interneurons. (**b,c**) Time-lapse images of Kikume Green-Red labeled interneurons immediately after photoconversion (**b**) and at the end of the experiment (**c**). The arrowhead indicates a cell migrating out of the MZ. Experiments were repeated over 10 different slices with similar results. (**d**) Cumulative frequency of migration speed for interneurons in the MZ (*n* = 48 cells). The dotted line represents the theoretical minimum speed required for migrating interneurons to leave the MZ during the experimental time (14 h). (**e**) Quantification of the fraction of cells at the MZ; *n* = 48 (theoretical), *n* = 141 (photo-converted) cells from 10 different slices; two-tailed Fisher's exact test, ***$p < 0.001$ ($p = 7.03$ e-8). (**f**) Schematic of experimental design for slice transplantation experiments. (**g,h**) Representative examples of slices following transplantation of MZ (**g**) and SVZ (**h**) derived interneurons. Asterisks indicate the original placement of transplanted cells. (**i**) Boxplots represent median, 1st and 3rd quartile, and 1.5 IQR for fraction of cells located in the MZ following transplantation of MZ and SVZ-derived interneurons. *n* =10 and12 slices, from 5 and 6 animals for MZ and SVZ derived cells respectively; two-tailed Student *t*-test, **$p < 0.01$ ($p = 4.545$ e-5). Scale bars equal 100 µm (**b,c**) and 200 µm (**g,h**).

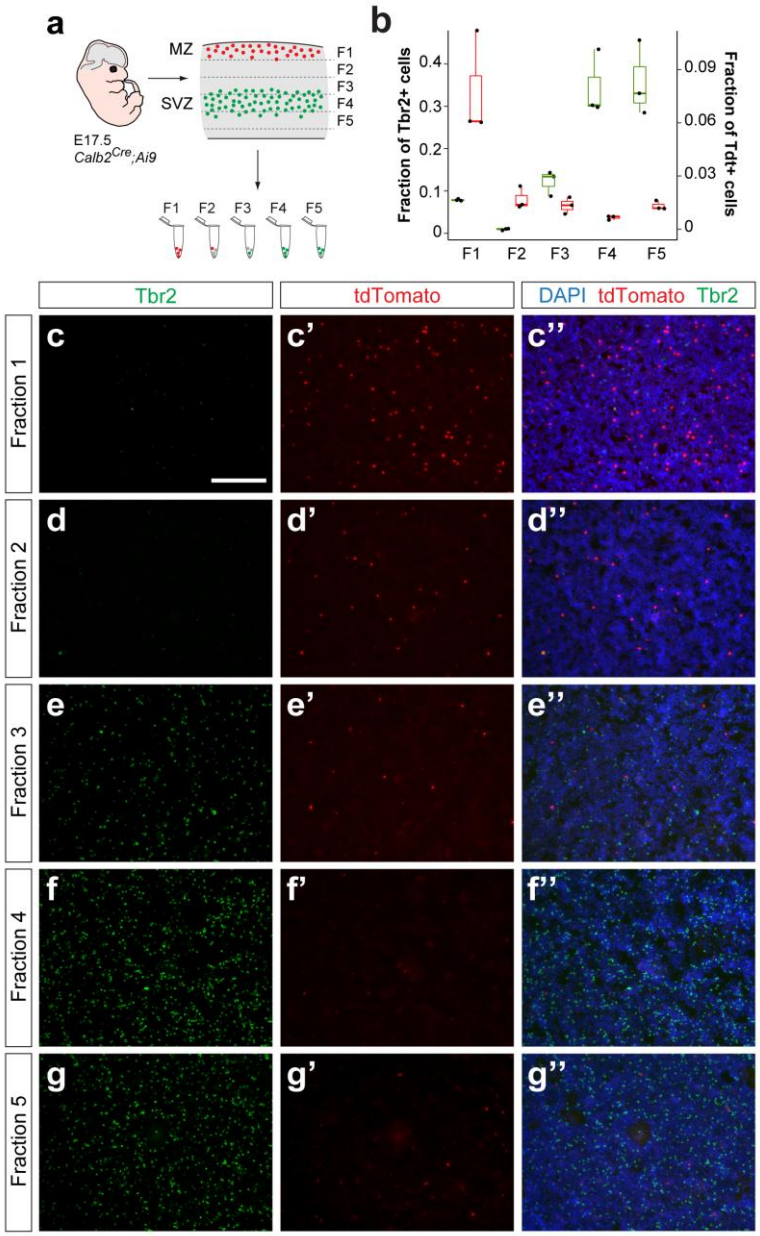

Supplementary Figure 3

Isolation of interneurons migrating through the MZ and SVZ.

(**a**) Schematic of experimental design for the isolation of neurons in progressively deeper positions of the embryonic cortex. (**b)** Boxplots represent median, 1st and 3rd quartile, and 1.5 IQR for percentage of TdTomato (CR+ cells) and Tbr2+ cells in each fraction, normalized to total cell number, n = 3 litters of embryos. (**c–g**) Representative images showing TdTomato (CR+ cells) and Tbr2+ cells in the different cellular fractions after dissociation and plating. Fraction 1 is closest to the pial surface and fraction 5 is closest to the ventricular zone (VZ). Experiments were repeated 3 times with similar results. Scale bar equals 200 µm.

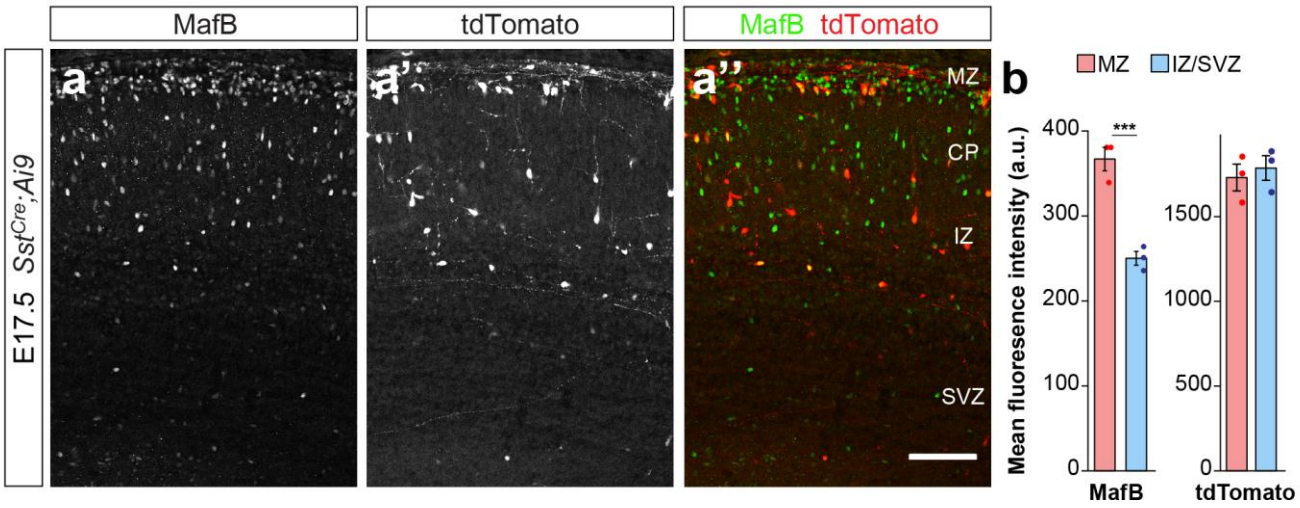

Supplementary Figure 4

MafB expression in migrating SST^{+} interneurons at E17.5.

(**a**) Coronal sections through the cortex of E17.5 from *Sst^{Cre};Ai9* mice showing expression of MafB (a and a'') in migrating SST+ interneurons (a' and a''), repeated over 3 animals with similar results (**b**) Quantification of mean fluorescence intensity for MafB in SST+/tdTomato+ cells migrating through the MZ or IZ/SVZ; n = 3 mice; one-way ANOVA; ***$p < 0.001$ ($p = 0.0004$ for MafB) and $p = 0.82$ (tdTomato). Histograms represent mean ± s. e. m. Scale bar equals 100 µm.

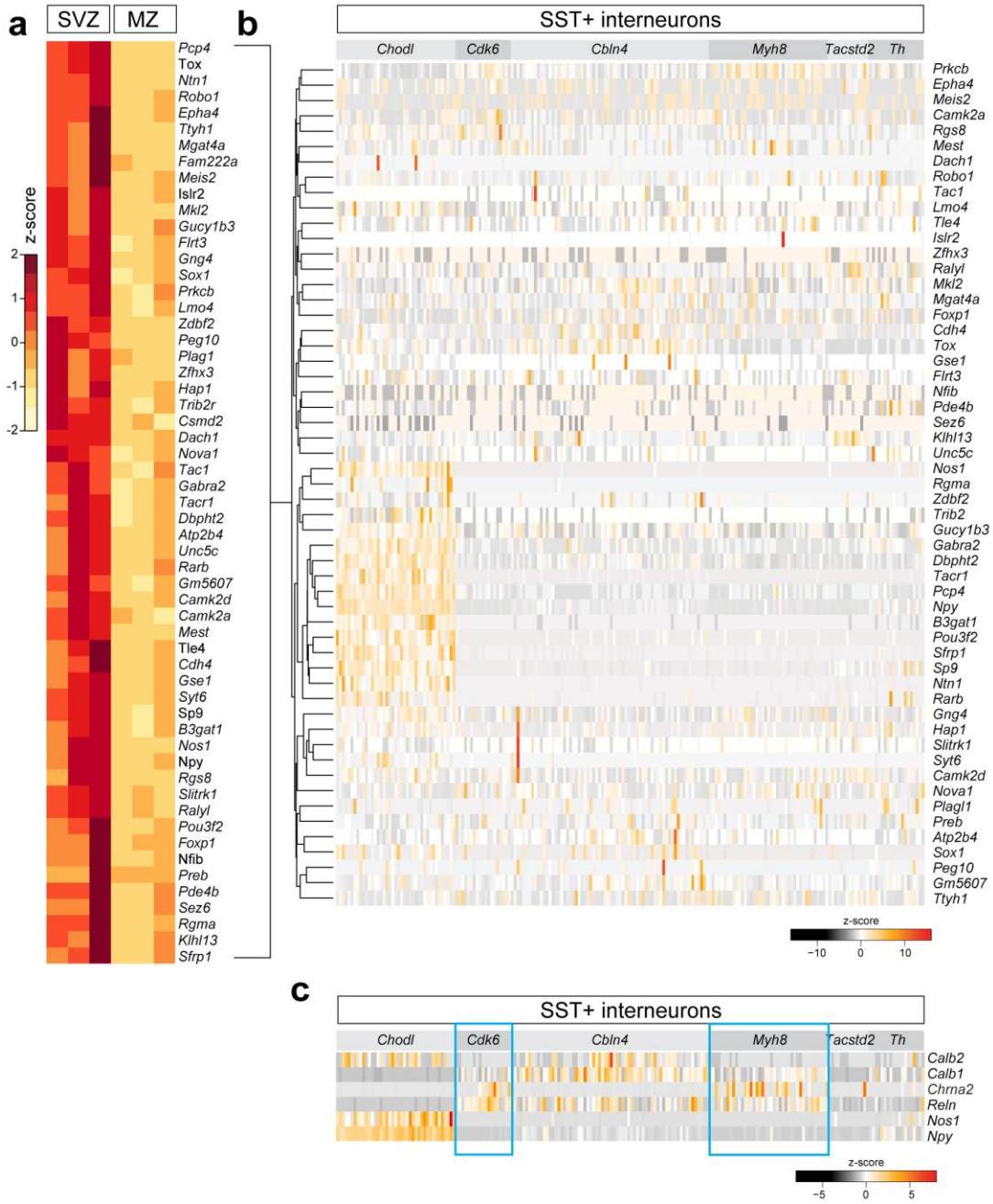

Supplementary Figure 5

Different classes of SST^{+} interneurons migrate through distinct routes.

(**a**) Heatmap representing relative levels (z-scores) of genes differentially enriched in SST+ cells migrating through the SVZ at E17.5, with FDR set at < 5% using the Benjamini-Hochberg method. (**b**) Heatmap representing relative levels (z-scores) of SVZ-enriched genes (from **a**) in different classes of SST+ interneurons from the adult visual cortex (data from Ref. 8). (**c**) Heatmap representing relative levels (z-scores) of genes expressed in different classes of SST+ interneurons from the adult visual cortex (data from Ref. 8). *Chrna2* appears to be preferentially expressed in Cdk6+ and Myh8+ populations of SST+ cells.

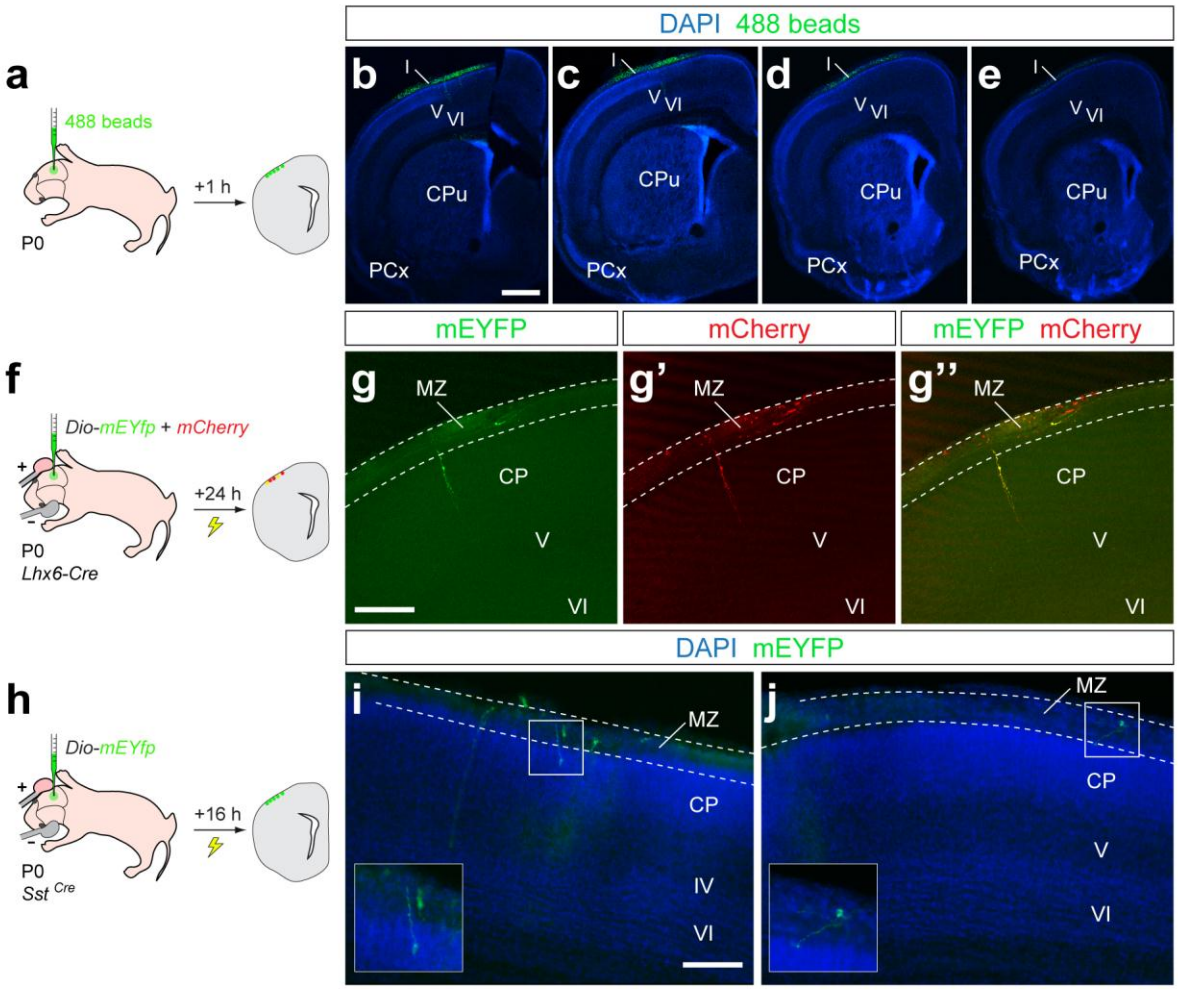

Supplementary Figure 6

Pial-surface electroporation targets cells migrating through the MZ.

(**a**) Schematic of experimental design for target injection in the MZ at birth. (**b–e**) Coronal sections through the telencephalon at P0 showing the extent of the distribution of Fluosphere Alexa 488 beads 1 h after injection, repeated 3 times with similar results (**f**) Schematic of experimental design for pial surface electroporation. (**g**) Coronal sections through the telencephalon 24 h after electroporation, repeated in 6 animals similar results. (**h**) Schematic of experimental design for pial surface electroporation. (**i,j**) Coronal sections through the telencephalon 16 h after electroporation, repeated over 5 animals with similar results. CP, cortical plate; CPu, caudoputamen nucleus; MZ, marginal zone; PCx, piriform cortex; V and VI, layers 5 and 6. Scale bars equal 200 µm (**b–e**) and 100 µm (**g,i,j**).

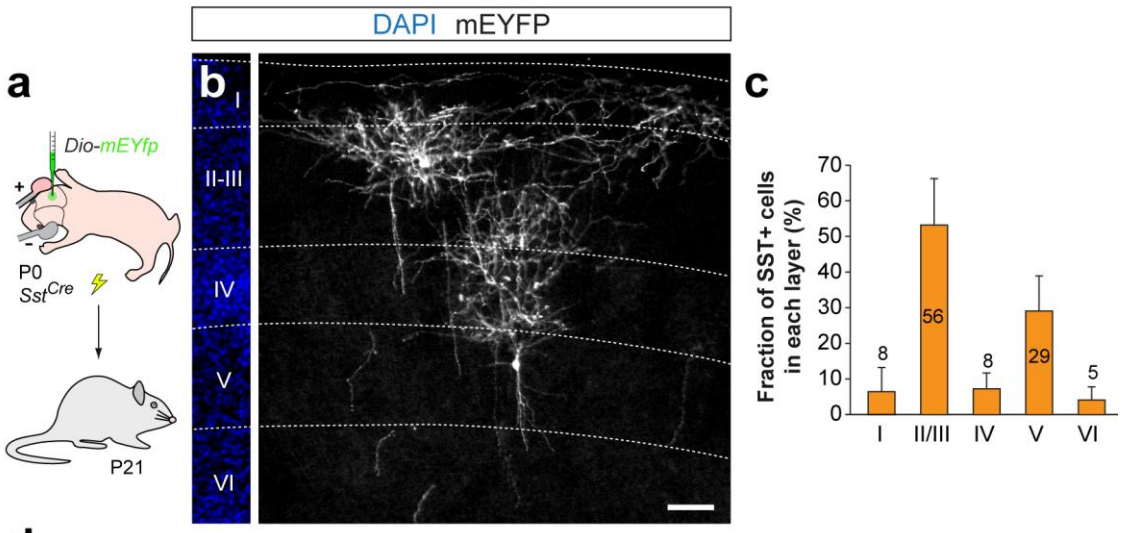

d

	Martinotti cell	Non-Martinotti	Martinotti %
L1	0	6	0%
L2/3	36	4	90%
L4	0	5	0%
L5	13	2	87%
L6	1	0	100%
total	50	17	75%

Supplementary Figure 7

Laminar distribution of SST$^+$ cells labeled using surface electroporation.

(**a**) Schematic of experimental design for pial surface electroporation in Cre-expressing neonates. (**b**) Coronal section through the cortex at P21 following pial surface electroporation at birth. (**c**) Quantification of the laminar distribution of SST+ interneurons at P21 following pial surface electroporation at birth, *n* = 106 cells from 15 animals. Error bars represent binomial proportion confidence interval. (**d**) Morphological description of surface electroporated cells. Scale bar equal 200 µm.

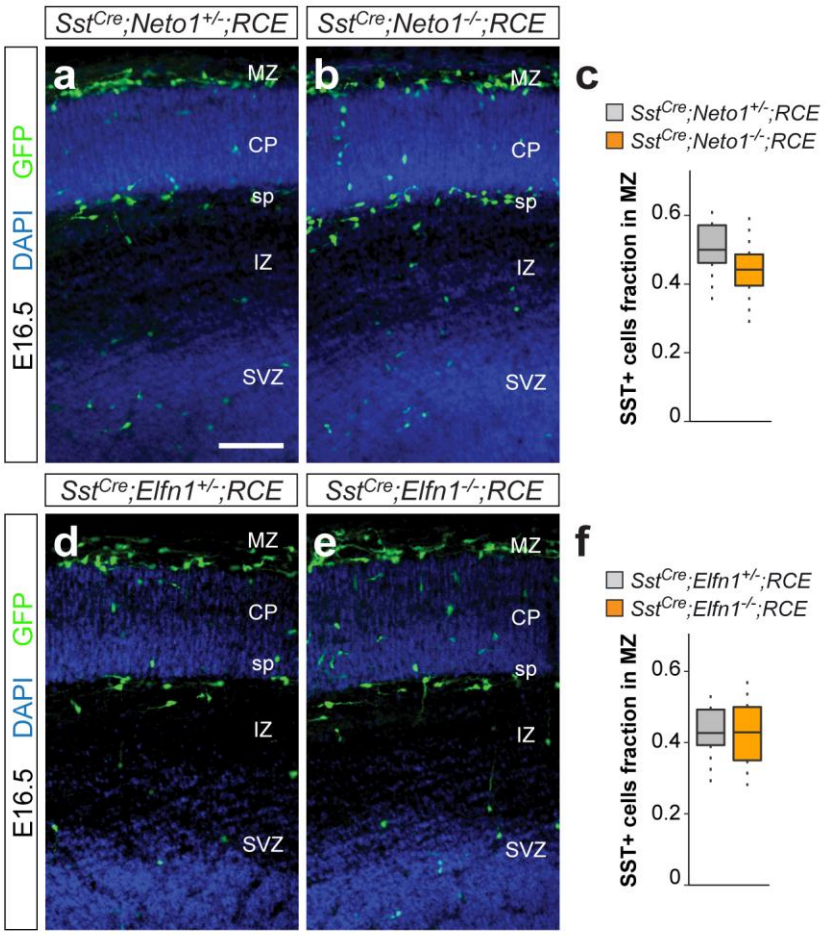

Supplementary Figure 8

Normal distribution of SST$^+$ migrating interneurons in *Neto1* and *Elfn1* mutants.

(**a,b,d,e**) Coronal sections through the cortex of E16.5 *Sst^{Cre};Neto1$^{+/-}$;RCE* (**a**), *Sst^{Cre};Neto1$^{-/-}$;RCE* (**b**), *Sst^{Cre};Elfn1$^{+/-}$;RCE* (**d**), and *Sst^{Cre};Elfn1$^{-/-}$;RCE* (**e**) mouse embryos, repeated over 3 mice per conditions with similar results. (**c,f**) Boxplots represent median, 1st and 3rd quartile, and 1.5 IQR for fraction of SST+ cells in the MZ; *n* = 11 sections per mice, 3 mice for each genotype; one-way ANOVA, *p* = 0.114 and *p* = 0.614, respectively. CP, cortical plate; MZ, marginal zone; SP, subplate; V and VI. Scale bar equals 100 µm.

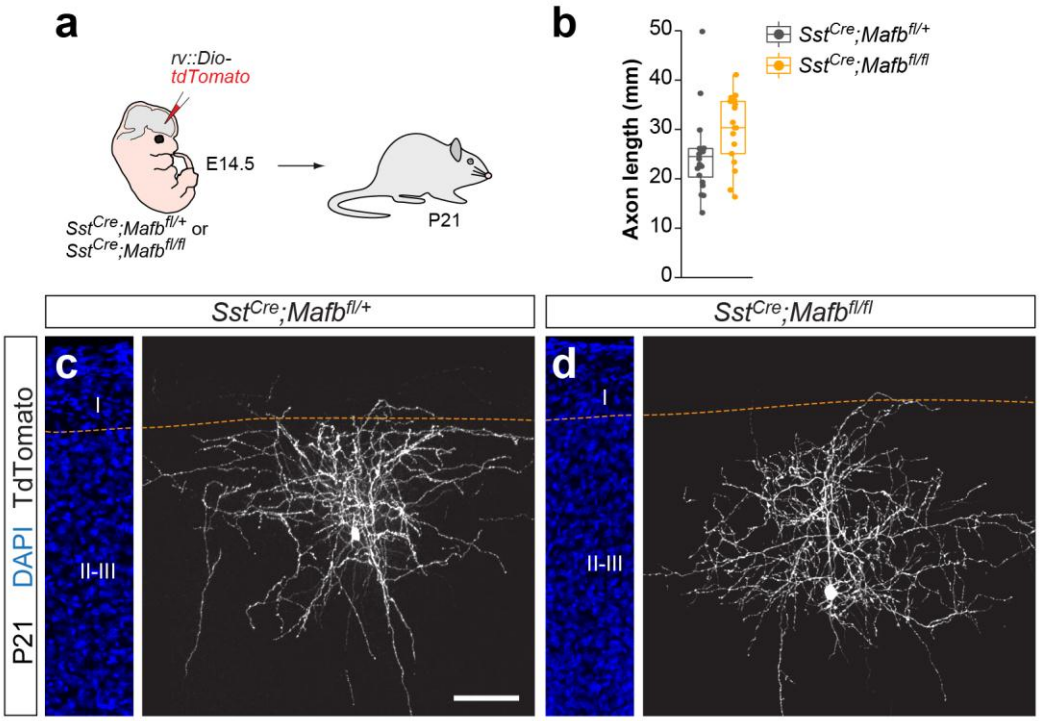

Supplementary Figure 9

Non-Martinotti SST^{+} cells have normal axonal length in conditional *Mafb* mutant mice.

(**a**) Schematic of experimental design for the labeling of interneuron progenitor cells using conditional retroviruses in Cre-expressing embryos. (**b**) Boxplots represent median, 1st and 3rd quartile, and 1.5 IQR for axonal length in non-Martinotti SST+ interneurons in layer 2/3, n = 23 and 17 cells from 8 and 10 mice of control and mutant genotype, respectively. Two-tailed Student *t*-test, $p = 0.87$. (**c,d**) Representative images of SST+ interneurons at P21 obtained through viral labeling at E14.5, repeated with similar results in 8 and 10 mice respectively. Scale bar equals 100 µm.

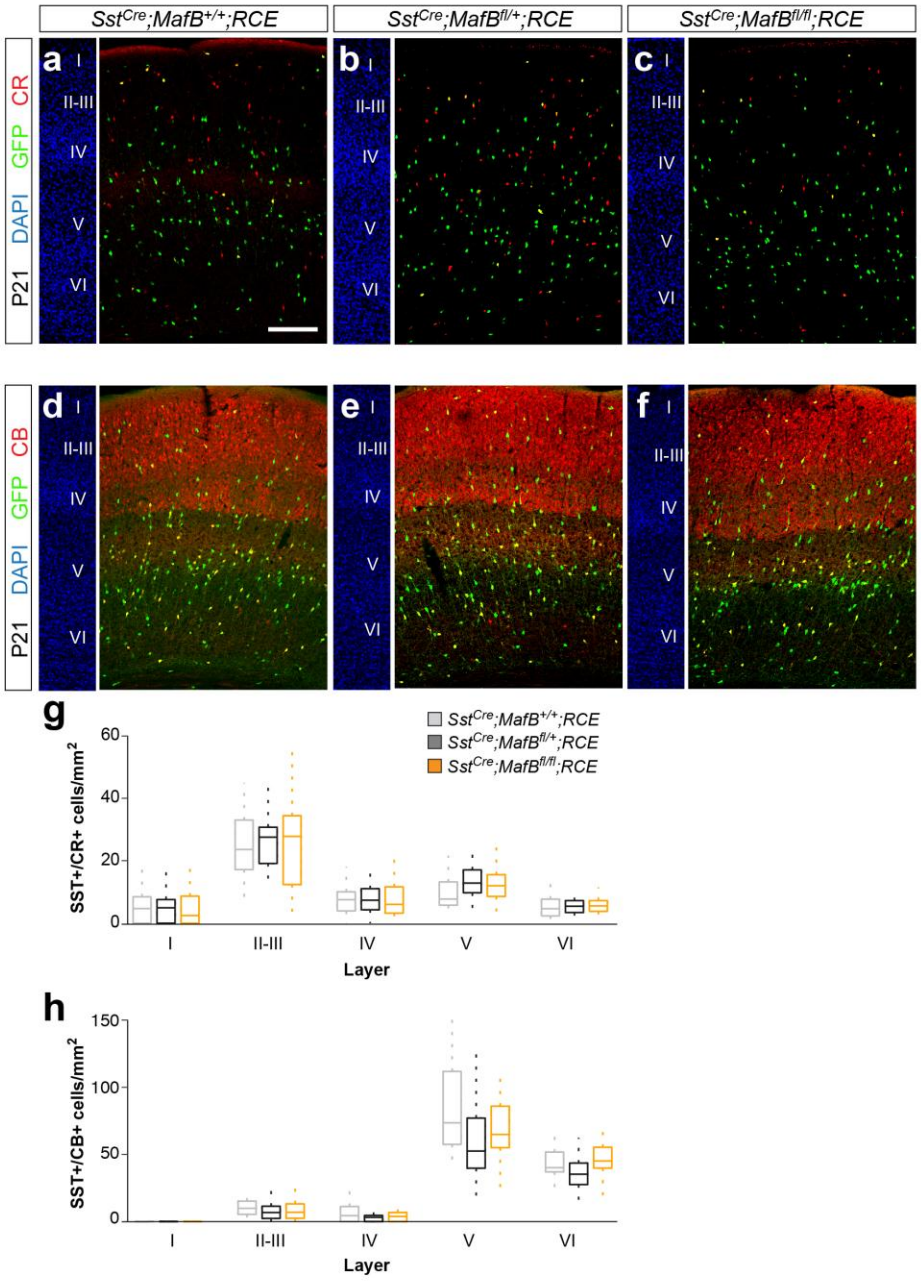

Supplementary Figure 10

Distribution of SST$^+$ and SST$^+$CR$^+$ interneurons in *Mafb* conditional mutants.

(**a–c**) Coronal sections through the somatosensory cortex of P21 *Sst^{Cre};Mafb$^{+/+}$;RCE* (**a, d**), *Sst^{Cre};Mafb$^{fl/+}$;RCE* (**b, e**), and *Sst^{Cre};Mafb$^{fl/fl}$;RCE* (**c, f**) mice showing expression of Calretinin (CR, **a–c**) and Calbindin (CB, **d–f**) in SST+ interneurons (GFP). (**g, h**) Quantification of the laminar distribution of SST+/CR+ (**g**) and SST/CB+ (**h**) cells for each genotype; *n* = 10 sections per animal, 3 mice per genotype; two-way ANOVA with post-hoc by Tukey HSD; *p* = 0.681 and *p* = 0.735 for CR and CB, respectively. Scale bar equals 100 µm.

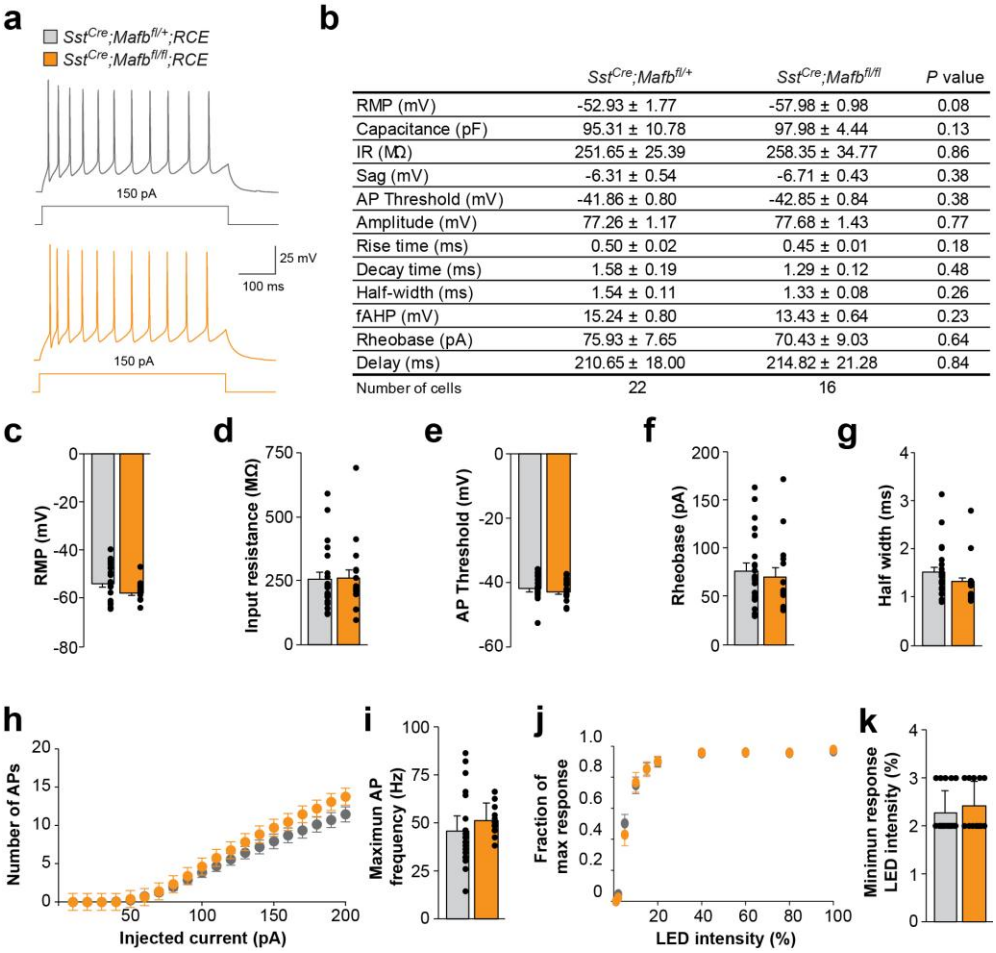

	$Sst^{Cre};Mafb^{fl/+}$	$Sst^{Cre};Mafb^{fl/fl}$	*P* value
RMP (mV)	-52.93 ± 1.77	-57.98 ± 0.98	0.08
Capacitance (pF)	95.31 ± 10.78	97.98 ± 4.44	0.13
IR (MΩ)	251.65 ± 25.39	258.35 ± 34.77	0.86
Sag (mV)	-6.31 ± 0.54	-6.71 ± 0.43	0.38
AP Threshold (mV)	-41.86 ± 0.80	-42.85 ± 0.84	0.38
Amplitude (mV)	77.26 ± 1.17	77.68 ± 1.43	0.77
Rise time (ms)	0.50 ± 0.02	0.45 ± 0.01	0.18
Decay time (ms)	1.58 ± 0.19	1.29 ± 0.12	0.48
Half-width (ms)	1.54 ± 0.11	1.33 ± 0.08	0.26
fAHP (mV)	15.24 ± 0.80	13.43 ± 0.64	0.23
Rheobase (pA)	75.93 ± 7.65	70.43 ± 9.03	0.64
Delay (ms)	210.65 ± 18.00	214.82 ± 21.28	0.84
Number of cells	22	16	

Supplementary Figure 11

Intrinsic properties of Martinotti cells in *Mafb* conditional mutants.

(**a**) Representative traces of voltage response to a depolarizing 150 pA current injection in layer 2/3 Martinotti cells from P21-28 $Sst^{Cre};Mafb^{fl/+};RCE$ and $Sst^{Cre};Mafb^{fl/fl};RCE$ mice. (**b**) Table showing intrinsic properties of layer 2/3 Martinotti cells from P21-28 $Sst^{Cre};Mafb^{fl/+};RCE$ and $Sst^{Cre};Mafb^{fl/fl};RCE$ mice. *p*-values calculated by two-tailed Mann-Whitney U test. Bar graph represents mean ± s.e.m., *n* = 22 and 16 cells, from 10 $Mafb^{fl/+};RCE$ and10 $Sst^{Cre};Mafb^{fl/fl};RCE$ mice, respectively. (**c-g**) Quantification of resting membrane potential (**c**), input resistance (**d**), action potential threshold (**e**), rheobase (**f**) and action potential half width (**g**). for (**c-g**), Bar graph represents mean ± s.e.m., *n* = 22 and 16 cells, from 10 $Mafb^{fl/+};RCE$ and10 $Sst^{Cre};Mafb^{fl/fl};RCE$ mice, respectively. (**h**) Number of action potentials evoked in response to increasing current injections in layer 2/3 Martinotti cells from P21-28 $Sst^{Cre};Mafb^{fl/+};RCE$ and $Sst^{Cre};Mafb^{fl/fl};RCE$ mice. Data is presented as mean ± s.e.m., *n* = 22 and 16 cells, from 10 $MafB^{fl/+};RCE$ and10 $Sst^{Cre};Mafb^{fl/fl};RCE$ mice, respectively (**i**) Bar graph represents mean ± s.e.m. of maximum action potential frequency evoked in layer 2/3 Martinotti cells from P21-28 ,*n* = 22 and 16 cells, from 10 $Mafb^{fl/+};RCE$ and10 $Sst^{Cre};Mafb^{fl/fl};RCE$ mice, respectively; two-tailed Student's T-test *p* = 0.30. (**j**) Fraction of the maximal response recorded from individual layer 2/3 pyramidal neurons following stimulation of ChR2-expressing SST+ cells in $Sst^{Cre};Mafb^{fl/+};RCE$ and $Sst^{Cre};Mafb^{fl/fl};RCE$ mice at increasing LED intensities. Data is presented as mean ± s.e.m., *n* = 19 and 12 cells 6 $Sst^{Cre};Mafb^{fl/+};RCE$ and 7 $Sst^{Cre};Mafb^{fl/fl};RCE$ mice, respectively. (**k**) Bar graph represents mean ± s.e.m. for of the minimal LED intensity required to evoke a detectable input in layer 2/3 pyramidal neurons from SST+ cells expressing ChR2, *n* = 19 and 12 cells from 6 $Sst^{Cre};Mafb^{fl/+};RCE$ and 7 $Sst^{Cre};Mafb^{fl/fl};RCE$ mice, respectively. Two-tailed Student's T-test, *p* = 0.39. RMP, resting membrane potential; Capacitance, membrane capacitance; IR, input resistance; Sag, h-current sag; AP Threshold, action potential threshold; Amplitude, action potential amplitude; Rise time, action potential rise time; Decay time, action potential decay time; Half width, action potential half width; fAHP, fast after-hyperpolarization amplitude; Delay, delay to first action potential.